Pion, kaon, and proton femtoscopy in Pb–Pb collisions at $\sqrt{s_{\rm NN}}$=2.76 TeV modeled in 3+1D hydrodynamics.

Adam Kisiel,[1,*] Mateusz Gałażyn,[1] and Piotr Bożek[2,3]

[1] *Faculty of Physics, Warsaw University of Technology, ul. Koszykowa 75, PL-00662, Warsaw, Poland*
[2] *AGH University of Science and Technology, Faculty of Physics and Applied Computer Science, al. Mickiewicza 30, PL-30059, Kraków, Poland*
[3] *The H. Niewodniczański Institute of Nuclear Physics, Polish Academy of Sciences, PL-31342 Kraków, Poland*

Femtoscopy is providing information on system size and its dynamics in heavy-ion collisions. At ultra-relativistic energies, such as those obtained at the LHC, significant production of pions, kaons and protons enables femtoscopic measurements for these particles. In particular the dependence of system size on pair momentum and particle type is interpreted as evidence for strong collective flow. Such phenomena are naturally modeled by hydrodynamics. We present calculations within the 3+1D hydrodynamic model coupled to statistical hadronization code THERMINATOR 2, corresponding to Pb–Pb collisions at $\sqrt{s_{\rm NN}}$ =2.76 TeV. We obtain femtoscopic radii for pions, kaons, and protons, as a function of pair transverse momentum and collision centrality. We find that an approximate universal scaling of radii with pair transverse mass and final state event multiplicity is observed, and discuss the consequences for the interpretation of experimental measurements.

PACS numbers: 25.75.-q, 25.75.Dw, 25.75.Ld
Keywords: relativistic heavy-ion collisions, femtoscopy, collective flow, transverse mass scaling

arXiv:1409.4571v1 [nucl-th] 16 Sep 2014

I. INTRODUCTION

The collisions of heavy-ions at ultra-relativistic energies have been studied at the Relativistic Heavy-Ion Collider (RHIC) at Brookhaven National Laboratory (BNL) for Au ions at $\sqrt{s_{\rm NN}}$ = 200 GeV. In the system created in such collisions the deconfined state of strongly-interacting matter is created, where the relevant degrees of freedom are quarks and gluons. It behaves as a strongly coupled liquid with small viscosity [1–4]. This behavior is well described by a variety of hydrodynamic codes, in terms of the transverse momentum spectra and the radial and elliptic flow phenomena, with the important addition of event-by-event fluctuations. While the behavior of the system is well understood in the momentum sector, its description in the space-time domain remained a challenge, and was achieved a few years ago [5, 6]. Based on these findings, hydrodynamic models were adapted to heavy-ion collisions at the highest currently available energy, achieved at the Large Hadron Collider (LHC) at CERN, for Pb ions with $\sqrt{s_{\rm NN}} = 2.76$ TeV.

One of the important cross-checks of the collective picture of the heavy-ion collision is the investigation of the space-time scales of the system, obtained via femtoscopy for pairs of identical particles. Such analysis is performed in the Longitudinally Co-Moving System (LCMS), where the the longitudinal direction is along the beam axis, the outwards direction is along the pair transverse momentum and the sidewards direction is perpendicular to the other two. Three independent sizes of the system in these directions (usually referred to as R_{long}, R_{out}, and R_{side} respectively, collectively called the "femtoscopic radii") are extracted as a function of event centrality and average pair transverse momentum $k_{\rm T} = |\boldsymbol{p_{\rm T,1}} + \boldsymbol{p_{\rm T,2}}|/2$. Both at RHIC and at the LHC a scaling was observed for these radii measured for pions, where they depended linearly on final state multiplicity $\langle dN_{ch}/d\eta \rangle^{1/3}$ and have a power-law dependence on $m_{\rm T} = \sqrt{k_T^2 + m_{\pi,K,p}^2}$ [7–13] A question arises if similar scaling is indeed observed for hydrodynamic models. In such calculations the hydro stage is usually followed by statistical hadronization, and subsequent resonance propagation and decay, as well as hadronic rescattering. Even if the scaling is observed at the end of the hydro stage, it is not obvious if it would still be observed after the hadronic stage. This work provides arguments to the discussion of such questions.

Hydrodynamic collectivity has a particular feature of involving all types of particles, including pions, kaons and protons, which are all subject to the same flow field. Therefore it is natural to expect that the scaling of radii will extend to results for heavier particles, such as kaons and protons. It can be shown analytically that a power-law scaling of the form $m_{\rm T}^{1/2}$ arises in a one-dimensional hydrodynamic expansion with negligible transverse flow and common freeze-out criteria [14, 15]. It is not known, if such scaling will still be present in state-of-the-art, fully three-dimensional calculations with significant transverse flow and viscosity, which are necessary to realistically model heavy-ion collisions. In addition the hadronic rescattering and resonance decays may have significantly different influence on different particle types. A recent realistic calculation including a hydro phase as well as hadronic rescattering phase suggests that the scaling between pions and kaons is broken at the LHC [16]. It

*Electronic address: kisiel@if.pw.edu.pl

is important to know, if this arises already at the hydro phase or if it is the effect of the hadronic rescattering. In the first case, the argument of the $m_{\rm T}$ scaling for radii for different particles as a signature of collectivity should be revisited. In the second case the experimental search for such a breaking would be an excellent probe for the length and importance of the hadronic rescattering phase at the LHC. In this work we perform the complete calculation for pions, kaons and protons in a model which includes the hydrodynamic phase as well as statistical hadronization and resonance contribution, but does not include hadronic rescattering. We discuss the consequences for the "$m_{\rm T}$ scaling as collectivity signature" argument.

Kaon and proton femtoscopy is significantly more challenging than the corresponding measurement for pions. As a consequence it is often done not in LCMS in three dimensions, but in a simplified way, in one dimension and in the Pair Rest Frame (PRF). We discuss what is the relation of the scaling of femtoscopic radii in LCMS and in PRF, and what kind of behavior is expected for one-dimensional radii for pions, kaons, and protons, measured as a function of pair $m_{\rm T}$.

The calculations presented in this work serve two purposes. Firstly, they represent predictions from 3+1-dimensional (3+1D) hydrodynamics + THERMINATOR 2 model for pion, kaon, and proton radii at the LHC as a function of event multiplicity and pair $m_{\rm T}$. Secondly, they calibrate an important probe of collectivity: the $m_{\rm T}$ dependence of femtoscopic radii, and give qualitative and quantitative predictions of how collectivity can be searched for with this measurement.

II. 3+1D HYDRO AND THERMINATOR 2 MODELS

A combination of two models is used in this work. The collective expansion is modeled in the 3+1D viscous hydrodynamics. The details of the implementation and the formalism of the model is presented in [17]. The calculation is coupled to the statistical hadronization and resonance propagation and decay simulation code THERMINATOR 2 [18].

The viscous hydrodynamic model evolves the flow velocity u^μ and energy density ϵ in 3+1D, following the second order Israel-Stewart equations [19]. The energy momentum tensor is composed of the ideal fluid part, the stress tensor $\pi^{\mu\nu}$ and the bulk viscosity correction Π

$$T^{\mu\nu} = (\epsilon + p + \Pi)u^\mu u^\nu - (p + \Pi)g^{\mu\nu} + \pi^{\mu\nu} \ . \qquad (1)$$

To obtain a realistic flow profile, important for the description of the femtoscopic radii, a hard equation of state should be used [5, 6]. We use a parametrizaton of the equation of state interpolating between lattice QCD results [20] at high temperatures and the hadron gas equation of state at low temperatures. For central rapidity region of heavy-ion collisions at the LHC, we set all chemical potentials to zero.

In this work we use smooth initial conditions for the hydrodynamic evolution. Event-by-event fluctuations in the initial conditions generate, after hydrodynamic evolution, fluctuating freeze-out hypersurfaces. It has been shown that these effects have negligible influence on the azimuthal angle averaged femtoscopy analysis [21]. The initial entropy density profile in the transverse direction is given by the Glauber model, as a combination of the density of participant nucleons ρ_{part} and binary collisions ρ_{bin} $\frac{1-\alpha}{2}\rho_{part} + \alpha\rho_{bin}$ with $\alpha = 0.15$. This choice of the initial density describes fairly well the centrality dependence of the charged particle density [22]. The detailed form of the entropy density profile in the longitudinal direction and the parameters can be found in Ref. [21]. The initial time for the hydrodynamic evolution is 0.6 fm/c, viscosity coefficients are $\eta/s = 0.08$ and $\zeta/s = 0.04$, and the freeze-out temperature $T_t = 140$ MeV. The calculation is performed for seven sets of initial conditions, corresponding to the given impact parameter b values (in fm) for the Pb–Pb collisions at the $\sqrt{s_{\rm NN}}$=2.76 TeV: 3.1, 5.7, 7.4, 8.7, 9.9, 10.9, and 11.9. They correspond, in terms of the average particle multiplicity density $\langle dN_{ch}/d\eta\rangle$, to given centrality ranges at the LHC [23]: 0-10%, 10-20%, 20-30%, 30-40%, 40-50%, 50-60%, and 60-70%. For completeness, some calculations have been also done for $b = 2.3$ fm corresponding to the 0-5% centrality range.

The freeze-out hypersufaces obtained in the hydro calculation are a direct input for the THERMINATOR 2 code, which performs a hadronization at these surfaces, with particle yields following the Cooper-Frye formula

$$E\frac{d^3N}{dp^3} = \int d\Sigma_\mu p^\mu f(p_\mu u^\mu) \ . \qquad (2)$$

$d\Sigma_\mu$ is the integration element on the freeze-out hypersurface and

$$f = f_0 + \delta f_{shear} + \delta f_{bulk} \qquad (3)$$

is the momentum distribution including nonequilibrium corrections. The hydrodynamic evolution generates the flow velocity at freeze-out, as well as the stress and bulk tensors, $\pi^{\mu\nu}$ and Π, necessary to calculate nonequilibrium corrections to the equilibrium distribution functions at freeze-out from shear viscosity

$$\delta f_{shear} = f_0\,(1 \pm f_0)\,\frac{1}{2T_f^2(\epsilon + p)}p^\mu p^\nu \pi_{\mu\nu} \qquad (4)$$

and bulk viscosity

$$\delta f_{bulk} = C f_0\,(1 \pm f_0)\left(\frac{(u^\mu p_\mu)^2}{3u^\mu p_\mu} - c_s^2 u^\mu p_\mu\right)\Pi \ , \qquad (5)$$

where c_s is the sound velocity and

$$\frac{1}{C} = \frac{1}{3}\sum_{hadrons}\int \frac{d^3p}{(2\pi)^3}\frac{m^2}{E}f_0\,(1 \pm f_0)\left(\frac{p^2}{3E} - c_s^2 E\right) \ . \qquad (6)$$

The THERMINATOR 2 model equates the chemical and kinetic freeze-out, and does not include the hadronic rescattering. Nonequilibrium terms (5) introduce corrections to particle rations, the effective chemical freeze-out temperature is higher than T_f [22]. All known resonances are used in the hadronization process. They are subsequently allowed to propagate and decay, in cascades if necessary. For every particle its creation point is either located on the freeze-out hypersurface (so-called "primordial" particles) or is associated with the point of the decay of the parent particle. This information is crucial for femtoscopic analysis performed in this work and is kept in the simulation.

III. FEMTOSCOPIC FORMALISM

The femtoscopic correlation function is a ratio of the conditional probability to observe two particles together, divided by the product of probabilities to observe each of them separately. Experimentally it is measured by dividing the distribution of relative momentum of pairs of particles detected in the same collision (event) by an equivalent distribution for pairs where each particle is taken from a different collision. The femtoscopy technique focuses on the mutual two-particle correlation, which can come from wave-function (anti-)symmetrization for pairs of identical particles. In this case the measurement is sometimes referred to as "Hanbury-Brown Twiss (HBT) correlations". Another source is the Final State Interaction (FSI), that is Coulomb or strong. At the moment no heavy-ion collision models exist that would take the effects of two-particle wave-function symmetrization or the FSI into account when simulating particle production. The effect is usually added in an "afterburner" code. This procedure is also used in this work. It requires the knowledge of each particles' emission point and momentum, which is provided by the THERMINATOR 2 model. We do not compare our correlation functions with the experiment directly, the comparison is only done at the level of the extracted femtoscopic radii. In the experimental analysis the FSI is usually a methodological complication, while the main physics observable is the correlation resulting from quantum statistics (QS) (anti-)symmetrization. Therefore in this work we simplify the "afterburner" calculation and only take into account the QS effect, the FSI is not taken into account. The procedure to extract the femtoscopic radii is modified accordingly and assumes that the only source of correlation is the QS. With this simplification the calculated radii can still be compared with experimental ones, while the systematic uncertainty on the calculation is reduced.

With such assumptions the correlation function can be expressed as:

$$C(\boldsymbol{k^*}) = \frac{\int S(\mathbf{r}^*, \boldsymbol{k^*})|\boldsymbol{\Psi}(\mathbf{r}^*, \boldsymbol{k^*})|^{\mathbf{2}}}{\int S(\mathbf{r}^*, \boldsymbol{k^*})} \tag{7}$$

where $\mathbf{r}^* = \mathbf{x_1} - \mathbf{x_2}$ is a relative space-time separation of the two particles at the moment of their creation. $\boldsymbol{k^*}$ is the momentum of the first particle in the PRF, so it is half of the pair relative momentum in this frame. S is the source emission function and can be interpreted as a probability to emit a given particle pair from a given set of emission points with given momenta. For identical bosons (pions and kaons), the wave function must be symmetrized and takes the form:

$$\Psi_{\pi,K} = 1 + \cos(2\boldsymbol{k}^* r^*) \tag{8}$$

while for the unpolarized fermions (protons), it is:

$$\Psi_p = 1 - \frac{1}{2}\cos(2\boldsymbol{k}^* r^*) \tag{9}$$

The calculation of the correlation function is as follows. First all particles of a certain type (charged pion, charged kaon, proton) from a THEMINATOR 2 event for a given centrality are combined into pairs. A histogram B is created where each pair is filled with the weight of 1.0, at a corresponding relative momentum $\boldsymbol{q} = 2\boldsymbol{k^*}$. The histogram can be one-dimensional (as a function of $|\boldsymbol{q}|$), three dimensional (as a function of three components of $\boldsymbol{q}$ in LCMS), or a set of one-dimensional histograms representing selected components of the spherical harmonic decomposition of the distribution [24]. The second histogram A is created, where the pair is inserted in the same manner, but with the weight calculated according to Eq. (8) for pions and kaons or Eq. (9) for protons. The correlation function C is calculated as A/B. Mathematically this procedure amounts to a Monte-Carlo calculation of the integral given in Eq. (7). The C obtained in this way closely resembles an experimental correlation function (modulo the absence of the FSI) and a standard experimental procedure to extract the femtoscopy radii from it can be applied. It is also identical to the procedure used in previous calculations based on the THERMINATOR model [17, 25, 26].

The correlation functions are then fitted to extract the femtoscopic radii, in a procedure designed to closely resemble the experimental one. First, the functional form of S is assumed to be a three-dimensional ellipsoid with a Gaussian density profile:

$$S(\boldsymbol{r}) \approx \exp\left(-\frac{r_{out}^2}{4R_{out}^2} - \frac{r_{side}^2}{4R_{side}^2} - \frac{r_{long}^2}{4R_{long}^2}\right), \tag{10}$$

where $r_{out,side,long}$ are components of r^* calculated in LCMS and R_{out}, R_{side}, and R_{long} are single-particle femtoscopic source radii. Then Eq. (7) gives the following fit function:

$$C(\boldsymbol{q}) = 1 + \lambda \exp\left(-R_{out}^2 q_{out}^2 - R_{side}^2 q_{side}^2 - R_{long}^2 q_{long}^2\right). \tag{11}$$

It can be directly fitted to the calculated correlation functions to extract the femtoscopic radii. Because of the simplifying assumption of not including the FSI in the calculation of the model function, there is no need

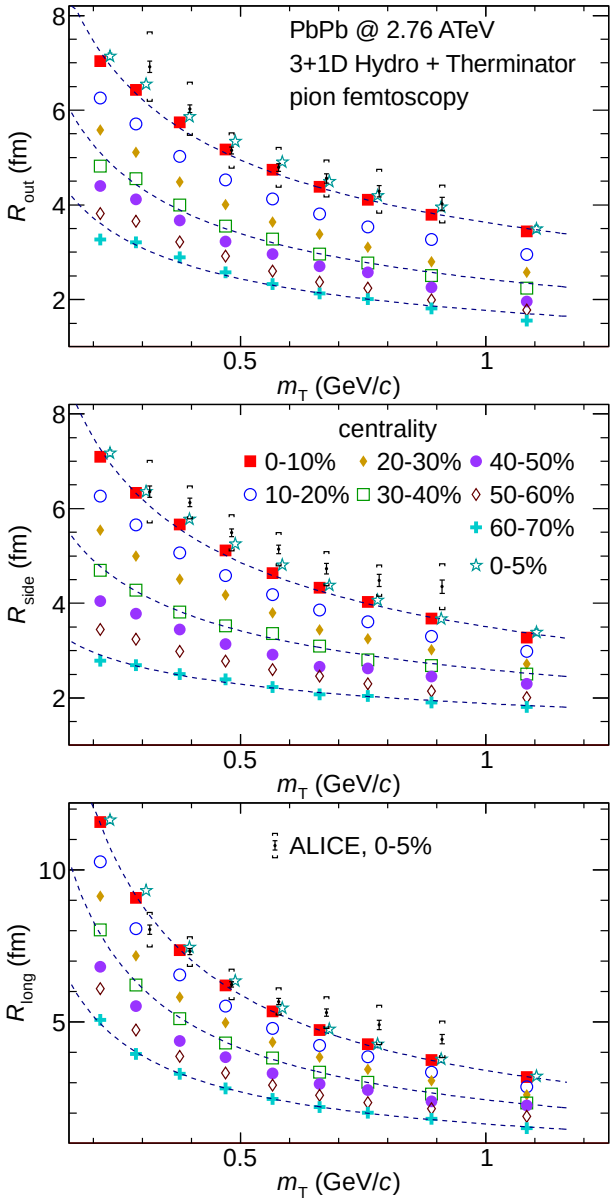

FIG. 1: Femtoscopic radii in LCMS calculated for pions, as a function of pair transverse momentum and centrality. Dashed lines show power-law fits to selected centralities. For completeness, calculations for $b = 2.3$ fm are compared to ALICE data [13] at the corresponding centrality. The two data sets are slightly shifted in x direction for visibility.

for additional factors accounting for them in the fitting function. The formula can be used directly for the three-dimensional function in Cartesian representation as well as in spherical harmonics decomposition. For one-dimensional correlation function a simplified source assumption is made:

$$S(\boldsymbol{r}^*) \approx \exp\left(-\frac{r^{*2}}{4R^2_{\rm inv}}\right), \qquad (12)$$

where the source is spherically symmetric in PRF with a single source size $R_{\rm inv}$. This gives the one-dimensional fit function:

$$C(q_{\rm inv}) = 1 + \lambda \exp\left(-R^2_{\rm inv} q^2_{\rm inv}\right). \qquad (13)$$

IV. SOURCE SIZES FOR PIONS, KAONS, AND PROTONS

The correlation functions are calculated separately for pions, kaons, and protons, for seven centrality ranges. The momentum dependence is studied by calculating the correlation function separately for pairs in the following $k_{\rm T}$ ranges (given in GeV/c): 0.1-0.2, 0.2-0.3, 0.3-0.4, 0.4-0.5, 0.5-0.6, 0.6-0.7, 0.7-0.8, 0.8-1.0, and 1.0-1.2 for pions. For kaons the $k_{\rm T}$ ranges start from 0.3, for protons from 0.4, since at lower momenta the multiplicity of the heavier particles is too limited to perform a reliable calculation. The given $k_{\rm T}$ ranges contain the significant part of the experimental acceptance at the LHC, in particular the acceptance of the ALICE experiment, which is the only one with advanced particle identification capabilities applicable in high multiplicity events on a particle-by-particle level. The calculation is intended as a test of the $m_{\rm T}$ scaling of radii for different particle types, therefore it is important that the $m_{\rm T}$ ranges for pions, kaons and protons overlap significantly.

In Fig. 1 the radii in LCMS for pions are shown as a function of centrality and $m_{\rm T}$. The transverse size reaches 7 fm for the lowest $m_{\rm T}$ and largest multiplicity events, the longitudinal size reaches over 11 fm in the same range. The lowest radii observed are on the order of 2 fm, for high $m_{\rm T}$ at the largest centrality. The calculations for $b = 2.3$ fm are in good agreement with data from top 5% central collisions from ALICE [13]. The radii universally fall with $m_{\rm T}$, in all directions and for all centralities. The lines, drawn for selected centralities, show fits of the power-law function:

$$f(m_{\rm T}) = \alpha m^{\beta}_{\rm T}, \qquad (14)$$

where α and β are free parameters. In all cases the power-law type function fits the radii dependence on $m_{\rm T}$ well. For the *out* radius, the β parameter is on the order of -0.45. For the *side* radius it is similar, however for the highest centrality it is closer to zero. For the *long* radius the slope is steeper, resulting in the β of -0.75, also slightly closer to zero for highest centrality. This behavior, known as the "lengths of homogeneity" mechanism [14, 27], is a signature of the collective flow of the system.

The radii universally grow with decreasing centrality (increasing event multiplicity), in all directions and at all $m_{\rm T}$. In Fig. 2 the same radii are re-plotted as a function of the final state multiplicity. The lines represent fits to the selected $m_{\rm T}$ ranges, linear in $\langle dN_{ch}/d\eta \rangle^{1/3}$. They show that the dependence is indeed universally linear in this variable, in all directions and at all centralities.

The two scalings mentioned above can be generalized with a common formula for all centralities and all $m_{\rm T}$,

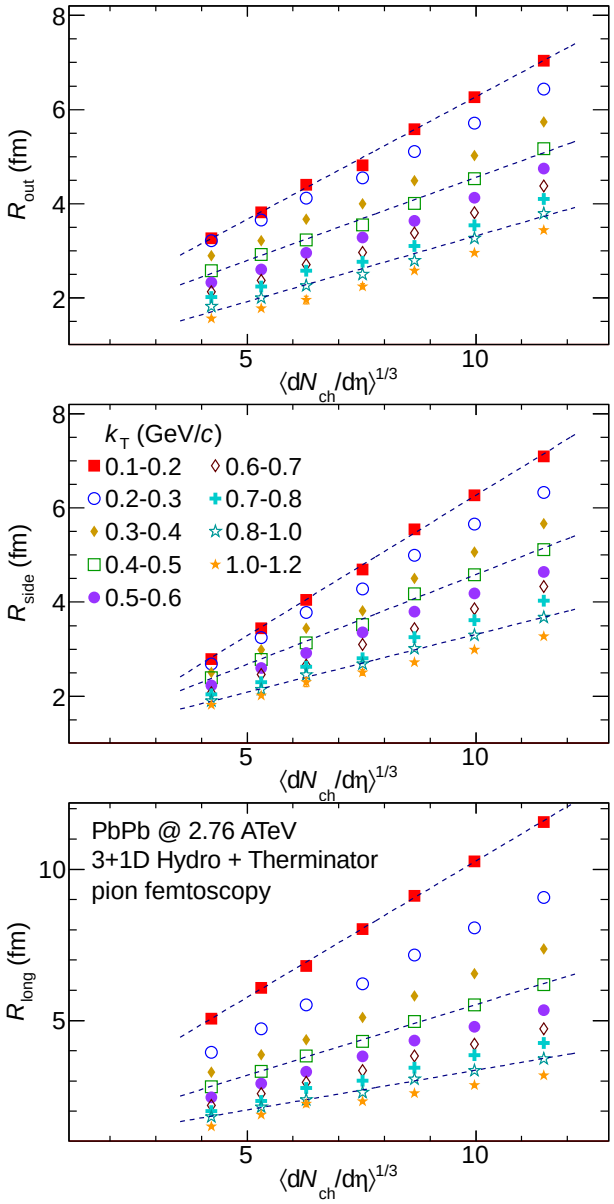

FIG. 2: Femtoscopic radii in LCMS for pions as a function of cube root of the charged particle multiplicity for several k_T ranges. Lines represent linear fits to selected k_T ranges.

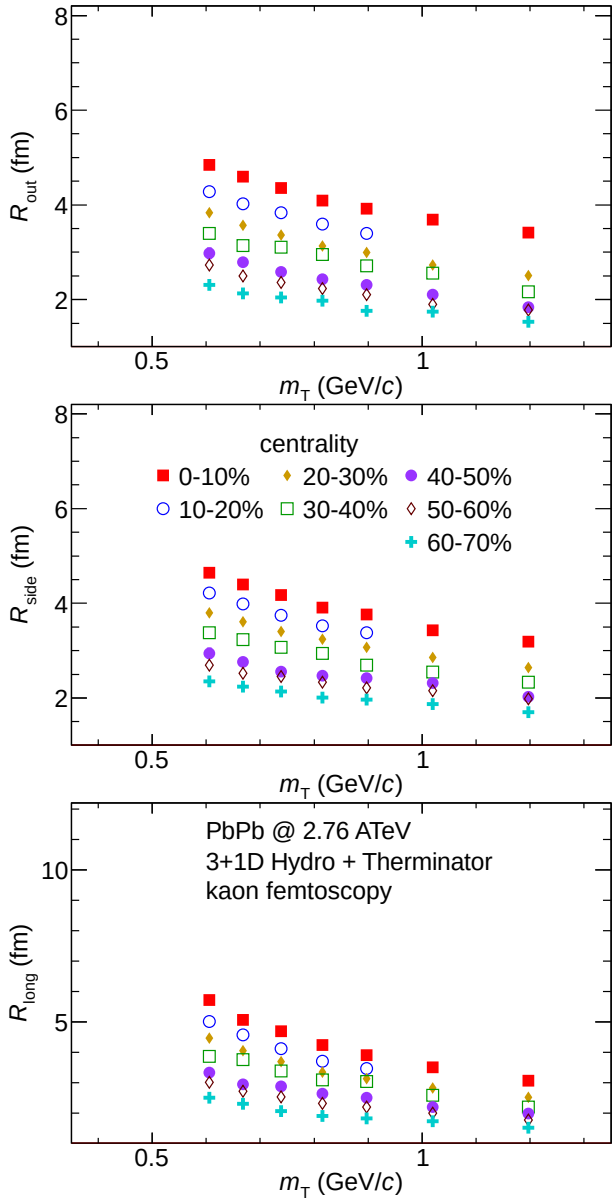

FIG. 3: Femtoscopic radii in LCMS calculated for kaons, as a function of pair transverse momentum and centrality.

given below:

$$R(x, y) = \alpha y^{\beta} (a + dx), \tag{15}$$

where y is m_T and x is $\langle dN_{ch}/d\eta \rangle^{1/3}$. The scaling holds to within 5% for R_{out}, R_{side}, and R_{long}, except for the highest centrality where deviations can reach 10% at high m_T. The parameters are: $\alpha = 1.98$, $\beta = -0.46$, $a = 0.33$, $d = 0.128$ for R_{out}, $\alpha = 2.00$, $\beta = -0.44$, $a = 0.29$, $d = 0.131$ for R_{side}, and $\alpha = 1.97$, $\beta = -0.78$, $a = 0.26$, $d = 0.130$ for R_{long}. α is similar for all radii, while β is larger in the *long* direction. The $\langle dN_{ch}/d\eta \rangle^{1/3}$ scaling parameters are similar in all directions. The scaling behavior shows that hydrodynamics produces common collective behavior in both transverse dimensions. The flow in the longitudinal direction has comparable features, but produces a steeper dependence on m_T, a consequence of a larger flow velocity.

The results for kaons are shown in Fig. 3. The kaon radii also decrease with m_T and increase with $\langle dN_{ch}/d\eta \rangle^{1/3}$. We have performed a fit with Eq. (15) to the kaon data and found that the radii follow the scaling with a comparable accuracy of 5%. The resulting parameters were the same as for the pion case, α on the order of 2.0, a on the order of 0.3 and d on the order of 0.13. Some difference was observed only for the β exponent, which was lower for kaons, -0.59 in *out*, -0.54 for *side*, and -0.86 for *long*. Taken at face value, the β parameter difference means that there is no common scaling of radii between pions and kaons. In reality, taking into account

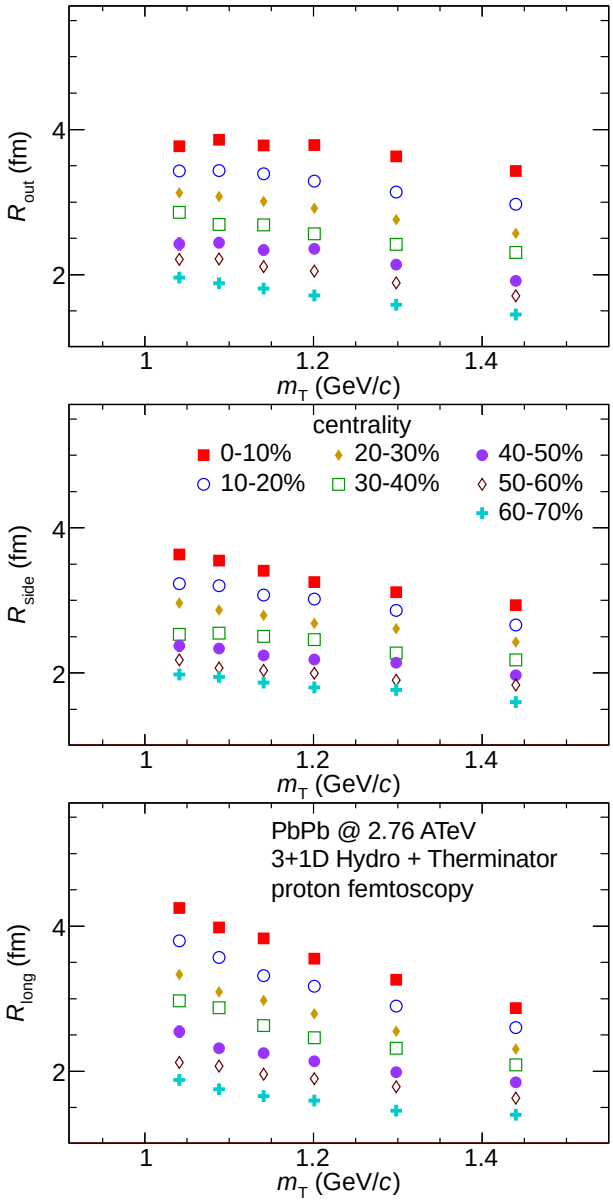

FIG. 4: Femtoscopic radii in LCMS calculated for protons, as a function of pair transverse momentum and centrality.

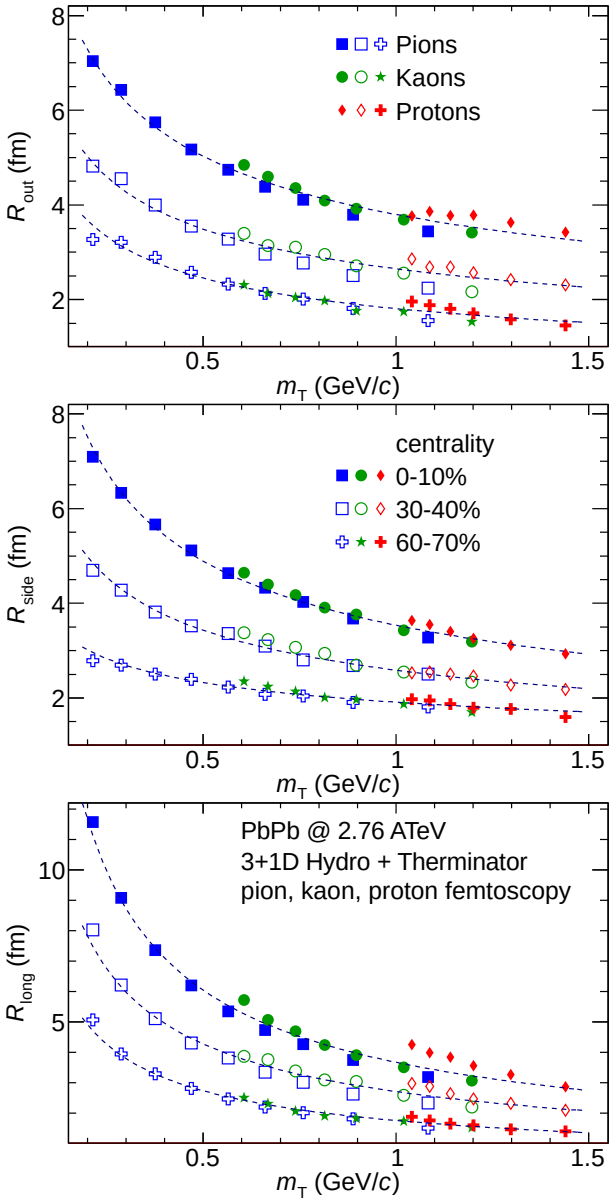

FIG. 5: Femtoscopic radii in LCMS for pions, kaons and protons, for selected centralities. Lines represent power-law fits to the combined pion, kaon, and proton data points at a given centrality and direction (see text for details).

the fact that experimental accuracy is seldom better than 5%, these values indicate that the common effective scaling between pions and kaons for radii vs. multiplicity and pair m_T exists. We will further test with what accuracy such statement can be made.

Finally, the results for protons are shown in Fig. 4. The proton radii also decrease with m_T and increase with $\langle dN_{ch}/d\eta \rangle^{1/3}$. We have performed a fit with Eq. (15) to the proton data and found that the radii follow the scaling with a comparable accuracy of 5%. The resulting parameters were the same as for pions and kaons, again the only parameter showing difference was the β exponent, which was even lower for protons, -0.58 in *out*, -0.61 for *side* and -1.09 for *long*. These values are again different than for the other particles, however close enough, so that an effective common scaling between pions and kaons vs. multiplicity and pair m_T may extend to protons as well.

In order to test the validity of such concept, the pion, kaon, and proton radii are plotted simultaneously as a function of m_T for selected centralities in Fig. 5. Each set of pion, kaon and proton radii for a given direction and centrality is then fit with a single function of the from given by Eq. (14). The fits are reasonable in all cases. We calculate the average absolute deviation of the results from the fitted curves. For the *out* direction they are 3%, 5% and 4% for the 0-10%, 20-30% and 60-70% centrality respectively. The β exponent is close to -0.42

for all cases. For the *side* direction the agreement of the fit is even better, with the average deviations of 2%, 2%, and 3% respectively. The β parameter varies more with centrality when compared to the *out* case, and is between 0.28 and 0.47. In the *long* direction the agreement of the fits improves as the centrality increases. The average deviation is 6%, 5%, and 3% for the three centralities. The β exponent is smaller than in *out* and *side*, as expected from previous calculations. It is -0.72 for the lowest and -0.64 for the highest centrality. In summary the plotted scalings, while not exact, are certainly realized with the accuracy of 5% for all directions, all centralities and the three particle types.

We also fitted all pion, kaon, and proton data points with a single function given in Eq. (15), for *out*, *side*, and *long* directions. For *out* and *side* this effective global scaling is obeyed at the 5% level, with a few outliers reaching 10%. In the *long* direction the scaling is obeyed to within 10%, with a few outliers reaching 20%. Therefore the minimal set of global parameters needed to approximately describe all pion, kaon, and proton data, for all centralities and all pair $m_{\rm T}$ are, for *out*: $\alpha = 2.11$, $\beta = -0.40$, $a = 0.32$, $d = 0.128$ for *side*: $\alpha = 2.04$, $\beta = -0.43$, $a = 0.42$, $d = 0.117$, and for *long*: $\alpha = 2.12$, $\beta = -0.68$, $a = 0.28$, $d = 0.133$.

With the given quality of the fits, comparable with the experimental uncertainties, we claim that the 3+1D Hydro + Therminator 2 simulation predicts an effective scaling of the three-dimensional femtoscopic radii in LCMS, common for pions, kaons and protons. The scaling has power-law like behavior as a function of pair $m_{\rm T}$, with similar exponents on the order of -0.4, in both transverse directions, while the exponent in the longitudinal direction is smaller, on the order of -0.7. The scaling is also linear in $\langle dN_{ch}/d\eta \rangle^{1/3}$, with the proportionality coefficient of 0.12 to 0.13. This scaling gives a powerful tool for the prediction of femtoscopic radii at any pair $m_{\rm T}$. We also see no reason why it should not extend to even heavier particles, such as Λ baryons.

Such a precise scaling was not observed in a recent calculation from the HKM model for pions and kaons [16]. There the kaon radii were predicted to be higher than the expected trend established for pions. It was not specified whether the scaling was broken already at the hydrodynamic stage of the model, or whether it arisen in the hadronic rescattering phase, modeled by UrQMD. Our study suggests that the latter scenario is true. It is therefore of great interest to test experimentally if such scaling exists. It will be a crucial test of the importance of hadronic rescattering phase in heavy-ion collisions at LHC.

V. SCALING IN ONE-DIMENSIONAL RADII

At LHC energies pions are most abundantly created particles, their multiplicities per-event are large enough for a precise measurement of pion femtoscopy in three

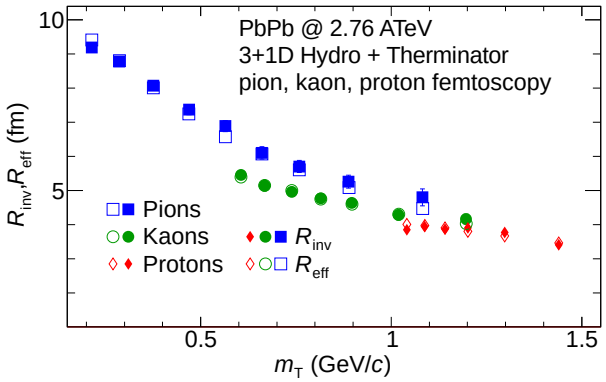

FIG. 6: Comparison of the $R_{\rm inv}$ obtained directly from the fit to the one-dimensional correlation function in PRF, and a result $R_{\rm eff}$ of the approximate procedure to estimate $R_{\rm inv}$ from values of $R_{\rm out}$, $R_{\rm side}$, and $R_{\rm long}$ measured in LCMS (see text for details).

dimensions and differentially in centrality and $m_{\rm T}$. However for heavier particles, such as kaons and protons statistics limitations arise. It is often possible to only measure one-dimensional radius $R_{\rm inv}$ for those particles. The measurement is then performed in the PRF. It is therefore interesting, in view of the effective scaling of the three-dimensional radii in LCMS shown above, to discuss similar scaling in PRF.

The transition from LCMS to PRF is a Lorentz boost in the direction of pair transverse momentum with velocity $\beta_{\rm T} = p_{\rm T}/m_{\rm T}$. Therefore only the $R_{\rm out}$ radius changes, becoming in PRF:

$$R^*_{\rm out} = \gamma_{\rm T} R_{\rm out}. \qquad (16)$$

where the value with asterisk is in PRF, and $\gamma_{\rm T}$ is the Lorentz factor of the transverse boost. The measured one-dimensional radius $R_{\rm inv}$ is a direction-averaged source size in PRF. According to Eqs. (12) and (13) it is the variance of the Gaussian source function. One than asks how does $R_{\rm inv}$ depend on the values of $R_{\rm out}$, $R_{\rm side}$, and $R_{\rm long}$? It is equivalent to the following mathematical problem: given the three random variables x, y, and z distributed with Gaussian probability density with variances R_x, R_y, and R_z respectively, what is the probability distribution of the variable $r = \sqrt{x^2+y^2+z^2}$? What is its Gaussian width R_i? Performing a simple calculation one finds that the probability density of r is Gaussian only in the special case of:

$$R_x = R_y = R_z. \qquad (17)$$

In all other cases it is not Gaussian and an exact formula for R_i does not exist. However if the variances in three dimensions are of the same order, the probability distribution of r is approximately Gaussian, and an "effective" radius can be estimated by fitting a Gaussian to the Monte-Carlo simulated distribution of r. This is equivalent to the "experimentalist" procedure of fitting the measured correlation function with the analytical for-

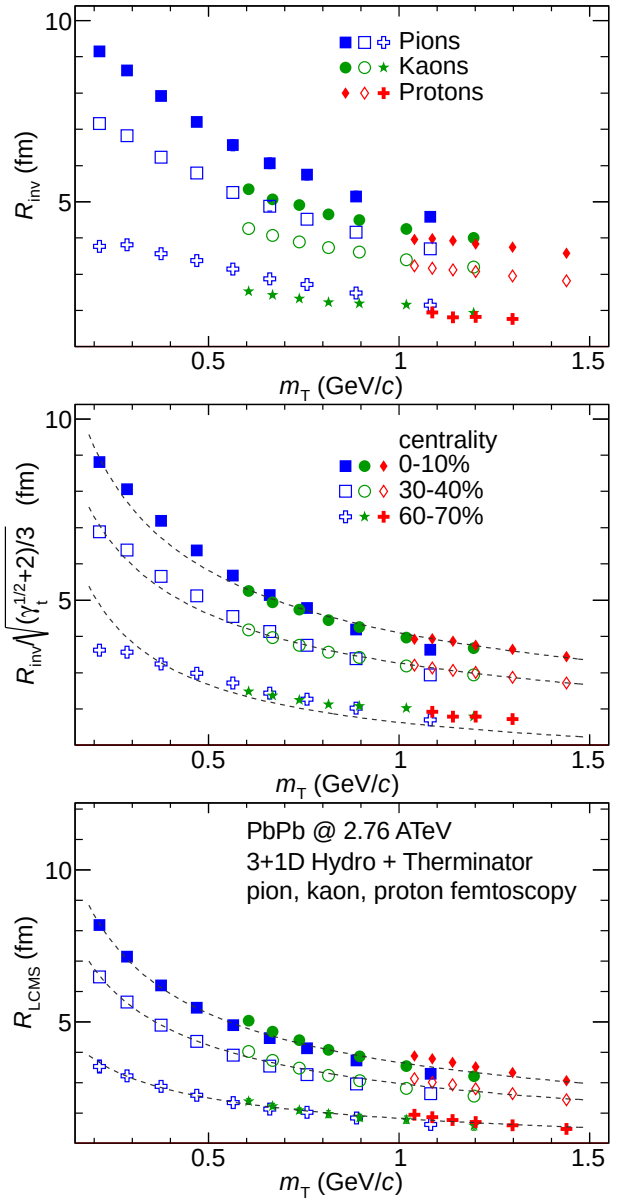

FIG. 7: Top panel: one-dimensional femtoscopic radius $R_{\rm inv}$ for pions, kaons, and protons calculated in the PRF for selected centralities. Middle panel: $R_{\rm inv}$ for pions, kaons, and protons scaled with the kinematic factor, for selected centralities (see text for details). Lines represent power-law fits. Bottom panel: Averaged one-dimensional radius in LCMS $R_{\rm LCMS}$ for pions, kaons, and protons for selected centralities. Lines represent power-law fits.

mula from Eq. (13), which implicitly assumes that the source is Gaussian.

We have tested this procedure for pions, kaons, and protons, the results are shown in Fig. 6. $R_{\rm inv}$ in the figure is obtained from a direct fit with Eq. (13) to the one-dimensional model correlation function in PRF. The effective radius $R_{\rm eff}$ is calculated, taking the corresponding $R_{\rm out}$, $R_{\rm side}$, and $R_{\rm long}$ from the fits performed in LCMS (discussed in the previous section) and applying the toy Monte-Carlo procedure described above. One can see a good agreement of both procedures, resulting in differences between both estimates not exceeding 3%. In other words the $R_{\rm inv}$value is directly and completely determined by the values of $R_{\rm out}$, $R_{\rm side}$, and $R_{\rm long}$in LCMS, as well as the corresponding Lorentz factor, coming from the pair velocity.

With that introduction one can proceed to predict the scaling of $R_{\rm inv}$ for pions, kaons, and protons, based on the LCMS results shown in the previous section. One immediately notices that for similar $m_{\rm T}$, the $\gamma_{\rm T}$ factor for pions will be very different than the one for kaons. A smaller, but still significant difference appears between the factors for kaons and protons at same $m_{\rm T}$. As seen in Fig. 5 the $R_{\rm out}$ for these three types of particles is similar at same $m_{\rm T}$, which means that R^*_{out} for pions, kaons, and protons will be different. That, in turn, means that $R_{\rm inv}$ for pions and kaons at same $m_{\rm T}$ will differ, and so will $R_{\rm inv}$ for kaons and protons at same $m_{\rm T}$. This is indeed clearly seen in top panel of Fig. 7, where $R_{\rm inv}$ values for pions, kaons, and protons show visibly different trends at any centrality.

We summarize the discussion above by saying that a common scaling of pion, kaon, and proton $R_{\rm inv}$ values *does not exist* (in our model), which is a trivial kinematic consequence of the *existence* of such scaling in three dimensions in LCMS. Moreover, the two scalings are mutually exclusive. As a consequence experimental values of $R_{\rm inv}$ for pions, kaons, and protons are not good observables in the validation of hydrodynamic collectivity predictions. For this purpose the correct observables are radii in LCMS, measured separately in the *out*, *side* and *long*.

We have argued that the violation of the scaling seen in the top panel of Fig. 7 is a consequence of the large differences in the Lorentz factor between pions, kaons, and protons at same $m_{\rm T}$. If that is the case, and the $R_{\rm out}$, $R_{\rm side}$, and $R_{\rm long}$ do scale separately between the three particle types, then the one-dimensional direction-averaged radius calculated in LCMS, $R_{\rm LCMS}$ should also scale. We have performed such calculation, which is shown in the bottom panel of Fig. 7, and indeed the approximate scaling is preserved, and still has a power-law like behavior.

We have verified that the violation of $R_{\rm inv}$ scaling has trivial kinematic origin. One might then ask, if it is possible to account for this known effect, and re-scale the measured $R_{\rm inv}$ for pions, kaons, and protons in such a way that they would be a good test of the hydrodynamic scaling. This would be experimentally much easier than performing a full three-dimensional analysis for kaons and protons, especially as a function of $m_{\rm T}$. We have found that when the radii are divided by the following scaling

factor [1]:

$$f = \sqrt{(\sqrt{\gamma_{\rm T}} + 2)/3}, \tag{18}$$

they fall back on a common curve (with the accurancy of 10%) for pions, kaons, and protons, which is shown in the middle panel of Fig. 7. However the power-law behavior of the scaling, seen still for $R_{\rm LCMS}$, is not preserved for the scaled $R_{\rm inv}$. We have therefore given a new "experimentalist" recipe for the search of hydrodynamic collectivity scaling between pions, kaons, and protons with the measurement of the one-dimensional radius in PRF.

VI. SUMMARY

We have presented calculations of femtoscopic radii for pions, kaons, and protons, as a function of centrality and pair $m_{\rm T}$. They were performed for the 3+1D hydrodynamic model coupled to the statistical hadronization, resonance propagation and decay code THERMINATOR 2. Hadronic rescattering was not included in the model. The radii were determined from the fits to the model correlation functions, closely following the experimentalist's recipe. We find that the radii show two effective scalings, which are independent of each other: a linear scaling in $\langle dN_{ch}/d\eta\rangle^{1/3}$ and a power-law like scaling in pair $m_{\rm T}$. These scalings exist separately in three dimensions in the LCMS frame. In the two transverse directions the $m_{\rm T}$ dependence is less steep (exponent -0.4) than in the longitudinal direction (exponent -0.7), while the $\langle dN_{ch}/d\eta\rangle^{1/3}$ scaling has similar slope in all directions. The scaling has common parameters for pions, kaons, and protons (with the accuracy of 5% to 10%). Other hydrodynamic calculations, which also included hadronic rescattering, found that such scaling is violated. Therefore an experimental verification of the existence of such scaling can serve as a probe for the importance of the hadronic rescattering phase.

We have also discussed similar scaling for one-dimensional radii measured in PRF. We have shown that the existence of the scaling for the three-dimensional radii in LCMS is mutually exclusive with the scaling for the radii in PRF between different particle types, due to trivial kinematic reasons. We propose that a measured $R_{\rm inv}$ is divided by a simple kinematic factor to recover the common effective $m_{\rm T}$ scaling for pions, kaons, and protons. In this way an experimentally simpler measurement of the one-dimensional radii for the three particle types can still be used as a probe for the hydrodynamic collectivity.

[1] For the discussion of the origin of the precise form of the factor, please see the Appendix

Acknowledgment

This work has been supported by the Polish National Science Centre under grants No. 2011/01/B/ST2/03483, 2012/07/D/ST2/02123, and 2012/05/B/ST2/02528.

Appendix

The form of the scaling factor for $R_{\rm inv}$ can be derived from the following discussion. In the ideal case given by the Eq. 17, the size $R_{\rm inv}$ corresponding to the variance of the variable r is known, and equal to the other sizes. Let us consider what will happen to the density distribution of r when we boost x with some Lorentz factor γ (corresponding to the boost of *out* from LCMS to PRF). It will certainly get broader, because x is now a wider distribution. A straightforward hypothesis is that R_i will grow as $(\gamma^2+2)/3$, since R_x will now be γR_x, and the averaging between the radii in three dimensions is done in quadrature. However Monte-Carlo simulations show that this is not the case. As γ grows, the x distribution becomes much wider than y and z. As a result, the distribution of r becomes somewhat wider, but also develops long non-Gaussian tails. Femtoscopy in this case is sensitive mostly to the width of the distribution near the peak, and these tails will have small influence on this width (they will have other consequences, such as lowering the λ parameter, but such discussion is beyond the scope of this paper). Therefore the R_i grows with γ, but slower then the naive expectation given above. We have found, through numerical simulations, that the actual growth is best described by the factor given by the Eq. (18), which has $\sqrt{\gamma}$ instead of the γ^2. The accuracy of such scaling is not better than 5%.

[1] J. Adams et al. (STAR), Nucl. Phys. **A757**, 102 (2005), nucl-ex/0501009.
[2] K. Adcox et al. (PHENIX), Nucl. Phys. **A757**, 184 (2005), nucl-ex/0410003.
[3] B. B. Back et al., Nucl. Phys. **A757**, 28 (2005), nucl-ex/0410022.
[4] I. Arsene et al. (BRAHMS), Nucl. Phys. **A757**, 1 (2005), nucl-ex/0410020.
[5] W. Broniowski, M. Chojnacki, W. Florkowski, and A. Kisiel, Phys.Rev.Lett. **101**, 022301 (2008), 0801.4361.
[6] S. Pratt, Nucl. Phys. **A830**, 51c (2009), 0907.1094.
[7] C. Adler et al. (STAR), Phys. Rev. Lett. **87**, 082301 (2001), nucl-ex/0107008.
[8] J. Adams et al. (STAR), Phys. Rev. **C71**, 044906 (2005), nucl-ex/0411036.
[9] S. S. Adler et al. (PHENIX), Phys. Rev. Lett. **93**, 152302 (2004), nucl-ex/0401003.
[10] B. Abelev et al. (STAR Collaboration), Phys.Rev. **C74**, 054902 (2006), nucl-ex/0608012.
[11] B. I. Abelev et al. (STAR), Phys. Rev. **C80**, 024905

(2009), 0903.1296.
[12] S. Afanasiev et al. (PHENIX Collaboration), Phys.Rev.Lett. **103**, 142301 (2009), 0903.4863.
[13] K. Aamodt et al. (ALICE Collaboration), Phys.Lett. **B696**, 328 (2011), 1012.4035.
[14] A. N. Makhlin and Y. M. Sinyukov, Z. Phys. **C39**, 69 (1988).
[15] Y. Sinyukov, Nucl.Phys. **A498**, 151C (1989).
[16] V. Shapoval, P. Braun-Munzinger, I. Karpenko, and Y. Sinyukov (2014), 1404.4501.
[17] P. Bozek, Phys.Rev. **C85**, 034901 (2012), 1110.6742.
[18] M. Chojnacki, A. Kisiel, W. Florkowski, and W. Broniowski, Comput.Phys.Commun. **183**, 746 (2012), 1102.0273.
[19] C. Gale, S. Jeon, B. Schenke, P. Tribedy, and R. Venugopalan, Phys. Rev. Lett. **110**, 012302 (2013), 1209.6330.
[20] S. Borsanyi et al., JHEP **11**, 077 (2010), 1007.2580.
[21] P. Bożek, Phys. Rev. **C89**, 044904 (2014), 1401.4894.
[22] P. Bożek and I. Wyskiel-Piekarska, Phys. Rev. **C85**, 064915 (2012), 1203.6513.
[23] K. Aamodt et al. (ALICE Collaboration), Phys.Rev.Lett. **106**, 032301 (2011), 1012.1657.
[24] A. Kisiel and D. A. Brown, Phys. Rev. **C80**, 064911 (2009), 0901.3527.
[25] A. Kisiel, W. Florkowski, and W. Broniowski, Phys. Rev. **C73**, 064902 (2006), nucl-th/0602039.
[26] A. Kisiel, W. Broniowski, M. Chojnacki, and W. Florkowski, Phys.Rev. **C79**, 014902 (2009), 0808.3363.
[27] S. V. Akkelin and Y. M. Sinyukov, Phys. Lett. **B356**, 525 (1995).